

## CONTENTS – K through L

---

Iron-Magnesium Diffusion Coefficients in Orthopyroxene: Implications for Metamorphism of the Petersburg Breccia <i>H. Kaiden and P. C. Buchanan</i> .....	5226
Different Radiation History of the CV3-type Carbonaceous Chondrites Allende, Coolidge, Ningqiong and Efremovka <i>L. L. Kashkarov and G. V. Kalinina</i> .....	5077
Impact Features from Vargeão Dome, Southern Brazil <i>C. Kazzuo-Vieira, A. P. Crósta, and A. Choudhuri</i> .....	5050
On the Origin of GEMS II: Spectrum Imaging of GEMS Grains in Interplanetary Dust Particles <i>L. P. Keller and S. Messenger</i> .....	5186
Fe-Ni Metal in LL3.0-6 Chondrites: Primordial and Secondary Features <i>M. Kimura and M. K. Weisberg</i> .....	5027
Mössbauer Mineralogy of Soils and Rocks at Meridiani Planum and Gusev Crater on Mars and Its Implications on the History of Water on Mars <i>G. Klingelhöfer, R. V. Morris, B. Bernhardt, D. Rodionov, S. Schröder, P. A. de Souza Jr., U. Bonnes, E. Evlanov, F. Foh, R. Gellert, P. Güttlich, E. Kankeleit, D. W. Ming, F. Renz, S. W. Squyres, T. Wdowiak, and A. Yen</i> .....	5231
Silverpit Structure, North Sea: Search for Petrographic and Geochemical Evidence for an Impact Origin <i>C. Koeberl and W. U. Reimold</i> .....	5156
Petrophysical Characteristic of Neuschwanstein EL-6 Chondrite <i>T. Kohout, F. Donadini, and L. J. Pesonen</i> .....	5079
Cooling Rate of Olivine Megacryst in the Yamato 980459 Olivine Phyric Shergottite <i>E. Koizumi, T. Mikouchi, M. Miyamoto, A. Monkawa, J. Chokai, and G. McKay</i> .....	5125
Detonation Nanodiamonds Instead of Stardust in Laboratory Simulation Experiments <i>A. P. Koscheev and U. Ott</i> .....	5144
Release of Noble Gases During Pyrolysis of Meteoritic and Synthetic Diamonds: A New Approach <i>A. P. Koscheev, M. D. Gromov, N. V. Zaripov, and U. Ott</i> .....	5137
Are Chondrules in the CB Carbonaceous Chondrite Gujba Primary (Nebular) or Secondary (Asteroidal)? <i>A. N. Krot, Y. Amelin, S. S. Russell, and E. Twelker</i> .....	5044
Oxygen Isotope Exchange in CAIs and Chondrules: Implication for Oxygen Isotope Reservoirs in the Solar Nebula <i>A. N. Krot, H. Yurimoto, I. D. Hutcheon, and E. R. D. Scott</i> .....	5043
Type C CAIs: New Insights into Early Solar System Processes <i>A. N. Krot, H. Yurimoto, M. I. Petaev, I. D. Hutcheon, and D. Wark</i> .....	5042
Condensation Origin Model for Chondrules <i>G. Kurat, M. E. Varela, E. Zinner, and A. Engler</i> .....	5070

World-Wide Impact Stratigraphy at the K-T Boundary: Implications for the Chicxulub Impact Angle <i>C. Lana and J. Morgan</i> .....	5063
Pseudotachylite-Fracture Network: A Key Structure for Central Uplift Formation in Large Impact Structures <i>C. Lana, R. Gibson, and U. Reimold</i> .....	5062
Corrosion of Solar-Composition Fe-based Alloys: First Results from the Nine Circles Experimental Cosmochemistry Laboratory <i>D. S. Lauretta</i> .....	5054
DUST-BUSTER Isotope TOF-MS for Stardust <i>T. Lee, W. F. Calaway, C. Y. Chen, J. F. Moore, M. J. Pellin, and I. V. Veryovkin</i> .....	5175
FeO-rich Xenoliths in the Staroye Pesyanoe Aubrite <i>C. A. Lorenz, M. A. Ivanova, G. Kurat, and F. Brandstaetter</i> .....	5014
Are Chondrites Older than Achondrites? The Tale of Al-26 <i>K. L. Lundgaard, M. Bizzarro, J. A. Baker, and H. Haack</i> .....	5135

**IRON-MAGNESIUM DIFFUSION COEFFICIENTS IN ORTHOPYROXENE: IMPLICATIONS FOR METAMORPHISM OF THE PETERSBURG BRECCIA**

H. Kaiden<sup>1,2</sup> and P. C. Buchanan<sup>1</sup>, <sup>1</sup>National Institute of Polar Research, Tokyo 173-8515, Japan. E-mail: kaiden@nipr.ac.jp. <sup>2</sup>Department of Polar Science, School of Multidisciplinary Sciences, The Graduate University for Advanced Studies, Tokyo 173-8515, Japan.

**Introduction:** The compositional zoning of minerals contained in igneous and metamorphic rocks provides us with clues about the thermal history of these rocks. Here, we report the results of modeling of the metamorphic redistribution caused by diffusion of iron at the edges of fragments of magnesian orthopyroxene in the polymict eucrite Petersburg. Previously [1], we suggested that this partial re-equilibration might have been caused by contact metamorphism. These calculations were made using two different sets of diffusion coefficients, which we initially suspected would provide different time periods for metamorphism. In fact, the results are quite similar.

**Calculations:** In the present study, we assumed that the compositional gradient of the mg# (=100 Mg/(Mg+Fe), molar) in these orthopyroxene fragments was controlled by atomic diffusion. In order to obtain cooling rates, diffusion profiles were numerically fit to the observed zoning profiles using calculation procedures similar to those in Miyamoto et al. [2]. Unfortunately, there are relatively few studies about Fe diffusion in pyroxene, and we were limited to the diffusion coefficients for orthopyroxene reported in [3] and [4].

**Results and Discussion:** One complicating factor of these calculations is that the diffusion coefficients for orthopyroxene suggested by these two studies [3, 4] vary with temperature. In the temperature range 1000 to 800 C, values are similar; however, at 500°C, the value suggested by [4] is nearly three orders of magnitude higher than that of [3]. We calculated the compositional profile resulting from Fe-Mg interdiffusion caused by cooling over the same temperature range (850 to 400 C) as [1] using the two sets of diffusion coefficients. The diffusion coefficients of [3] give the best fit profile at a cooling rate of 0.16 C/year (a period of ~3000 years), and the diffusion coefficients of [4] give the best fit profile at a cooling rate of 0.25 C/year (~2000 years).

**Conclusions:** Despite significant differences in the suggested diffusion coefficients at low temperatures [3, 4], the calculated cooling rates are very similar and are within the range expected for wall rock near a laccolith intruded into the crust of 4 Vesta [1]. This similarity in calculated zoning profiles suggests that diffusion at maximum temperatures during metamorphism is the most important factor in determining the character of the zoning profile in the orthopyroxene fragments in Petersburg.

**References:** [1] Buchanan P. C. and Kaiden H. 2004. Abstract #1502. 35th Lunar & Planetary Science Conference. [2] Miyamoto M. et al. 1986. *Journal of Geophysical Research* 91:12804–12816. [3] Ganguly J. and Tazzoli V. 1994. *American Mineralogist* 79:930–937. [4] Miyamoto M. and Takeda H. 1994. *Journal of Geophysical Research* 99:5669–5677.

**DIFFERENT RADIATION HISTORY OF THE CV3 -  
TYPE CARBONACEOUS CHONDRITES ALLENDE,  
COOLIDGE, NINGQIONG AND EFREMOVKA.**

L. L. Kashkarov and G. V. Kalinina. V. I. Vernadsky  
Institute of Geochem. and Analyt. Chem. Russian Acad. of  
Science. 119991, Kosygin str. 19, B-334, Moscow, Russia.  
*ugeochem@geochem.home.chg.ru*

The early pre-accretion stage of the chondrite parent  
body formation is one of the mostly important in the  
history of these meteorites [1-4].

The carbonaceous low-metamorphic chondrites  
Allende CV3 (sample N 15035), Coolidge CV3 (N 2566),  
Ningqiong CV3 (N 15855) and Efremovka CV3 (N 2349)  
have been studied with help of the track method. Track  
results obtained for the about 1300 olivine micro crystals  
(higher ~30  $\mu\text{m}$  and up to 150  $\mu\text{m}$  in size) were separated  
from the bulk meteorite samples are the following: (1) The  
total spread of the measured track density ( $\rho$ , track/cm<sup>2</sup>)  
values for all these meteorites is in the interval of five  
orders of magnitude  $\sim(10^3 - 10^8)$ ; (2) Statistical track  
density distribution in each meteorite under investigation  
indicate some specific peculiarities: in Allende only 9% of  
crystals have  $\rho = 10^6$  in comparison to the rest which  
demonstrate  $\rho = 10^4$ ; however, it is not observed any  
crystals with very low  $\rho$  values in the Coolidge, Ningqiong  
and Efremovka, in which the intervals for  $\rho$  amount  
comparatively narrow intervals equal to  $\sim(10^6 - 10^7)$ ,  $\sim(10^5$   
 $- 10^6)$  and  $\sim(10^7 - 10^8)$ , correspondingly; (3) In all these  
meteorites were observed crystals (not higher than 1%)  
with track density gradient that indicate on exposure of this  
matter by heavy ( $23 < Z < 28$ ) solar cosmic ray nuclei in the  
absence of the thin shielding layer of material.

Obtained results indicate on the differing radiation  
histories of these meteorite parent body (ies) formation on  
the early pre-compaction stage.

This work was supported by grant 04-05-64930 from  
RFFI.

**References:**[1] Kashkarov L.L. 1995. 26<sup>th</sup> Lunar and  
Planetary Science Conference. pp. 727-728. [2] Kashkarov  
L.L. 1995. Radiation Measurements 25:311-314. [3]  
Kashkarov L.L. et al. 2000. Geochemistry International  
38:Suppl. 3, S310-S321. [4] Kashkarov L.L. and Ustinova  
G.K. 2000. 31<sup>st</sup> Lunar and Planetary Science Conference.  
CD-ROM, N1046.

## IMPACT FEATURES FROM VARGEÃO DOME, SOUTHERN BRAZIL

C. Kazzuo-Vieira<sup>1</sup>, A. P. Crósta<sup>1</sup> and A. Choudhuri<sup>1</sup>. <sup>1</sup>Geosciences Institute, Univ. Campinas, Brazil. E-mail: alvaro@ige.unicamp.br

**Introduction:** Vargeão Dome is a 12.4 km diameter circular depression located in southern Brazil. It was formed on Cretaceous basalts and Jurassic/Triassic sandstones. Since it was first reported in 1978, several hypotheses have been proposed to explain its origin: alkaline intrusion [1], volcanic crater [2] and impact by an extraterrestrial body [3][4]. Although the impact hypothesis has been widely accepted, little evidence has been given. In this paper, we describe a wide set of impact features recently found at Vargeão.

**Geological Setting and Impact Features:** The Vargeão circular structure was formed on basaltic rocks of Serra Geral Formation and sandstones of the Pirambóia (Triassic) and Botucatu (Jurassic) formations, all units of the Paraná basin. Outside the structure, there are no occurrences of Jurassic/Triassic sandstones at the surface. Boreholes drilled for oil in the region found these sandstones at depths from 700 to 1,000m, below several layers of basaltic flows. However, in the central portion of the structure, highly deformed blocks of sandstones crop out, bounded by faults.

The analysis of aerial photographs, Landsat-7/ETM+ imagery and digital elevation model led to the recognition of two types of structures. The first type, on a regional scale, is characterized by a sub-rectangular system, controlled by two patterns of fractures/faults, with directions N70-60E and NW. The second occurs only within the structure, characterized by an annular-radial system, formed as a result of collapse faulting and the development of the central uplift, during the modification stage of crater formation.

Impact breccias found in Vargeão include two major types: monomict breccias comprising diabase and basalt; polymict breccias with fragments of sandstone, basalt, diabase and mudstone. Most of the breccias occur in concentric plateaus in the inner portion of the structure, within and around the central uplift.

Uplift in the center of the structure seems to have reached some hundreds of meters, as indicated by the current position of the sandstones. Erosion may also have played a role in exposing the sandstones at the present surface. However, the topographic gradient of 150m between the crater rim the adjacent inner portions of the crater floor, together with gradients of 70m between the central uplift and its surroundings, indicate that the original crater morphology is partially preserved.

Shatter cones were found in sandstones and basalts in several locations within and around the central uplift, with individual cones reaching up to 50cm in sandstones and 12cm in basalts.

Petrographic analysis of brecciated sandstones and basalts revealed abundant planar deformation features (shock lamellae) in quartz and plagioclase, with up to 4 crystallographic directions.

**Conclusion:** The recognition of a wide set of impact features indicates that Vargeão Dome was formed by the impact of an extraterrestrial body at a still undetermined time, but after the formation of basaltic lava flows of the Serra Geral Fm. (post 120 Ma.)

**References:** [1] Paiva Filho et al. 1978. *XXX Cong. Bras. Geol.*, Brazilian Geol. Soc., 408-412. [2] Barbour Jr. E. et al. 1981. *Paulipetro – relatório Técnico, Consórcio CESP-IPT*. [3] Crósta A. P. 1982. *XXXII Cong. Bras. Geol.*, Brazilian Geol. Soc., 1372-1377. [4] Hachiro J. et al. 1993. 3<sup>o</sup> Simp. Geol. Sudeste, Brazilian Geol. Soc., 276-283.

**ON THE ORIGIN OF GEMS II: SPECTRUM IMAGING OF GEMS GRAINS IN INTERPLANETARY DUST PARTICLES.** L. P. Keller and S. Messenger. Mail Code SR, NASA Johnson Space Center, Houston, TX 77058.

**Introduction:** GEMS (glass with embedded metal and sulfides) are enigmatic grains – they are a major component of primitive anhydrous interplanetary dust particles (IDPs) – and although a few % are demonstrably presolar [1], most GEMS grains are isotopically solar and chemically distinct from inferred interstellar grain compositions [2]. Previously, we proposed that most GEMS grains (~80%) were formed in the early solar nebula while the remaining GEMS have bulk compositions consistent with an interstellar origin [2]. We have quantitatively mapped individual GEMS grains in order to determine whether their internal elemental distributions will shed more light on their origin.

**Samples:** We used a JEOL 2500SE 200 keV field-emission scanning-transmission electron microscope (TEM) equipped with a thin window energy-dispersive X-ray (EDX) spectrometer to obtain spectrum images of several GEMS in ultramicrotome thin sections of three IDPs: L2011B10, L2011\*B6, and U2073A5B. Each pixel of a spectrum image contains a full EDX spectrum, enabling the determination of quantitative element abundances on the scale of individual pixels. Spectrum images of GEMS grains were acquired with a 4 nm incident probe whose dwell time was minimized to avoid beam damage and element diffusion during mapping. Successive image layers of each GEMS grain were acquired and combined in order to achieve ~5% counting statistics for major elements (e.g. Mg, Si, S, and Fe) in each pixel.

**Results and Discussion:** We mapped the elemental distributions of 10 GEMS grains. No “relict” crystalline grains were observed in the cores of any of the mapped GEMS grains similar to those previously reported [3]. However, some GEMS grains in brightfield TEM images are revealed to be aggregates of smaller GEMS in spectrum images. GEMS grains are compositionally heterogeneous on the ~20 nm scale. Core-to-rim zoning profiles are observed for Mg and Ca, but are generally not symmetric (a similar result was obtained by [4]). We have also observed oscillatory zoning of Al and Ca. Fe in GEMS occurs as Fe metal and FeS inclusions and is incorporated in the amorphous silicate matrix. Nanophase Ni-rich metal occurs in S-rich GEMS (decorated with FeS grains) – these Ni rich grains (10 nm) are likely by-products of sulfidization reactions of FeNi metal in the early solar nebula as proposed by [2]. It has been suggested that GEMS precursors were FeS and forsterite that were subject to intense radiation processing [3], but we found no examples of GEMS with FeS-rich cores, nor have we observed GEMS with Mg-rich cores (GEMS with Mg/Si > 1.5 are rare).

**Conclusions:** The observed compositional heterogeneity in these GEMS is unlikely to have resulted from extensive radiation processing, which would tend to homogenize their elemental distributions *via* ion-mixing [e.g. 5]. The observed heterogeneities may reflect the primary formation conditions of GEMS through the accretion of compositionally distinct subgrains or through condensation/shock processes which can produce compositional differences at this scale [6].

**References:** [1] Messenger, S. et al., (2003) *Science*, 300, 105. [2] Keller, L. P. and Messenger, S. (2004) *LPSC XXXV*, #1985. [3] Bradley, J. P. (1994) *Science*, 265, 925. [4] Joswiak, D. et al. (1996) *LPSC 27*, 625. [5] Cheng, Y. et al. (1991) *Proc. MRS*, 201, 75. [6] Keller, L. P. and McKay, D. S. (1997) *GCA* 61, 2331.

**FE-NI METAL IN LL3.0-6 CHONDRITES: PRIMORDIAL AND SECONDARY FEATURES.**

M. Kimura<sup>1</sup> and M. K. Weisberg<sup>2,3</sup>, <sup>1</sup>Faculty of Science, Ibaraki University, Mito 310-8512, Japan, <sup>2</sup>Dept. Physical Sciences, Kingsborough College, City University of New York, Brooklyn, NY 11235, <sup>3</sup>Dept. Earth and Planetary Sciences, American Museum of Natural History, NY, NY 10024, U.S.A.

**Introduction:** The composition of Fe-Ni metal in ordinary chondrites is a useful indicator of chemical group and petrologic type [e.g., 1]. Here we report the results of our systematic study of Fe-Ni metal in two LL3.0, six LL3.1-3.9, and three LL4-6 chondrites. We suggest that the characteristic features of Fe-Ni metal are highly sensitive not only to thermal metamorphism, but also to host chondrule chemistry.

**Fe-Ni metal in Semarkona:** Fe-Ni metal in Semarkona (LL3.0) chondrules generally shows plessitic intergrowths [2], and its composition varies widely. We obtained the average bulk chemical composition of metal in each chondrule by defocused electron beam microanalysis. The Cr and P contents of the metal are positively related to the mg ratio (Mg/Mg+Fe) of the host chondrule bulk composition. This observation suggests that these minor elements were incorporated into the metal during chondrule formation, supporting the results of previous studies (e.g., [3]). On the other hand, the bulk metal composition shows a positive correlation between Ni (4.0-9.1%) and Co (0.21-0.46%), and the Ni content is not correlated with the mg ratio of the host chondrule. We suggest that the variation in Ni and Co contents in chondrule metal reflects its primordial composition prior to chondrule formation. Some chondrule metal contains low-Ni (1.3-2.2% in bulk composition) and low-Co (0.10-0.12%), reflecting reduction processes.

Although Ni and Co-rich metal is rarely reported in LL3 chondrites [e.g., 1, 2], we found that metal composition depends on its occurrence. Fe-Ni metals on chondrule surfaces and as isolated grains in the matrix are highly enriched in Ni (51.8-68.5%) and Co (0.7-3.4%), and are generally surrounded by troilite and magnetite. This indicates that Ni and Co-rich metal formed by sulfidation and/or oxidation, similar to some metal in CR and other chondrites [4].

**Fe-Ni metal in LL3.0-6:** Fe-Ni metal in Y74660 (LL3.0) chondrules does not show plessitic intergrowths, but metal in the matrix is enriched in Ni (51.9-64.1%) and Co (0.29-1.84%). On the other hand, in LL3.1 to 6 chondrites, kamacite has higher Co content than taenite, in spite of its occurrence, as previously reported [e.g., 1, 5, 6]. This reflects metamorphic modification. We conclude that only the Fe-Ni metal in LL3.0 chondrites, especially Semarkona, preserves the primordial features it acquired during or before chondrule formation. Therefore, metal composition is one of the most sensitive indicators for distinguishing type 3.0 chondrites from higher petrologic subtypes.

**References:** [1] Afittalab F. and Wasson J.T. 1980 *GCA*, 44, 431-446. [2] Reisener R.J. and Goldstein, J.I. 1999 Abstract #1868. *30th Lunar & Planetary Science Conference*. [3] Zanda. B. et al. 1994 *Science*, 265, 1846-1849. [4] Weisberg M.K. et al. 1990 *Meteoritics*, 25, 269-279. [5] Nagahara H. 1982 *Mem. Natl. Inst. Polar Res.*, 25, 86-96. [6] Kimura M. et al. 2003 *Meteorit. Planet. Sci.*, 38, A33.

### MÖSSBAUER MINERALOGY OF SOILS AND ROCKS AT MERIDIANI PLANUM AND GUSEV CRATER ON MARS AND ITS IMPLICATIONS ON THE HISTORY OF WATER ON MARS

G. Klingelhöfer<sup>1,2</sup>, R. V. Morris<sup>1,4</sup>, B. Bernhardt<sup>1,2</sup>, D. Rodionov<sup>1,2,3</sup>, C. Schröder<sup>1,2</sup>, P. A. de Souza Jr.<sup>1,5</sup>, U. Bonnes<sup>10</sup>, E. Evlanov<sup>3</sup>, F. Foh<sup>1</sup>, R. Gellert<sup>1,2,9</sup>, P. Gütlich<sup>1,2</sup>, E. Kankeleit<sup>1,10</sup>, D.W. Ming<sup>4</sup>, F. Renz<sup>1,2</sup>, S. W. Squyres<sup>8</sup>, T. Wdowiak<sup>1,7</sup>, A. Yen<sup>1,6</sup>.

<sup>1</sup>MIMOS II Consortium, <sup>2</sup>Johannes Gutenberg-Universität, Inst. Anorganische & Analytische Chemie, Mainz, Germany, klingel@mail.uni-mainz.de. <sup>3</sup>Space Research Institute IKI, Moscow, Russia. <sup>4</sup>NASA Johnson Space Center, Houston, TX, USA. <sup>5</sup>CVRD Group, Vitoria, Brazil. <sup>6</sup>Jet Propulsion Laboratory, California Institute of Technology, Pasadena, CA, USA. <sup>7</sup>University of Alabama, Birmingham, AL, USA. <sup>8</sup>Cornell University, Ithaca, NY, USA, <sup>9</sup>MPI Cosmochemistry, Mainz, Germany, <sup>10</sup>Darmstadt University of Technology, Darmstadt, Germany.

**Introduction:** The Mars-Exploration-Rovers (MER) Spirit at the Gusev Crater landing site and Opportunity at the Meridiani Planum landing site are both carrying the Mössbauer spectrometer MIMOS II, which is part of the Athena instrument suite consisting of remote sensing instruments [1], and the In-Situ instruments mounted on an robotic arm (IDD): (i) Rock Abrasion Tool (RAT), (ii) Mössbauer (MB) spectrometer Mimos II [2], (iii) Microscopic Imager [1], and (iv) Alpha Particle X-ray Spectrometer (APXS) [3]. The IDD instruments are used to determine the chemistry and mineralogy of rocks and soils.

**MIMOS II Mössbauer results:** The MB results on rocks at the Gusev crater landing site show a primarily olivine-basalt composition. For some of the rocks a weathering rind has been detected using the RAT and subsequently APXS and MIMOS II. Magnetite has been identified in both soils and rocks at Gusev. All rock and soil spectra at Gusev are dominated by the mineral signature of olivine.

The Meridiani Planum landing site looks very different from Gusev crater. Opportunity landed inside a shallow crater (Eagle crater), with an outcrop covering part of the crater interior close to the rim. Mössbauer measurements show that this outcrop material consists predominantly of the Fe-sulfate jarosite, hematite, and a basaltic component (olivine, pyroxene). The same material was found again a couple of hundred meters away at the small crater Fram suggesting that the whole area is covered with this jarositic material. This strongly supports the presence of large amounts of water at this site in the past. The plains and a large portion of Eagle crater are covered by spherules with a diameter of several mm up to about 1 cm. Mössbauer data clearly show that the composition of these spherules (called 'Blueberries') is dominated by the Fe-oxide hematite. How these berries formed is still open. The composition of the soil at Meridiani is found to be basaltic, dominated by olivine similar to the Gusev site. An isolated rock close to Eagle crater (called Bounce rock) was determined by MB to be completely composed of Fe-2+ pyroxene. The data look very similar to some of the SNC meteorites. These results are supported by the APXS data [3,4].

Funded by the German Space Agency DLR and NASA, USA.

**Reference:** [1] Squyres S. W. et al. (2003), *J. Geophys. Res.*, 108(E12), 8062, doi:10.1029/2003JE002121. [2] Klingelhöfer et al. *J. Geophys. Res.*, 108(E12), 8067, doi: 10.1029/2003JE002138, 2003. [3] Rieder et al. *J. Geophys. Res.*, 108(E12), 8066, doi:10.1029/2003JE002150. [4,] Zipfel J. et al. (2004) this issue. [5,] Rodionov D. et al. (2004) this issue.

**SILVERPIT STRUCTURE, NORTH SEA: SEARCH FOR PETROGRAPHIC AND GEOCHEMICAL EVIDENCE FOR AN IMPACT ORIGIN.**

Christian Koeberl<sup>1</sup> and W. Uwe Reimold<sup>2</sup>. <sup>1</sup>Department of Geological Sciences, University of Vienna, Althanstrasse 14, A-1090 Vienna, Austria (christian.koeberl@univie.ac.at); <sup>2</sup>Impact Cratering Research Group, School of Geosciences, University of the Witwatersrand, Johannesburg 2050, South Africa (reimoldw@geosciences.wits.ac.za).

Stewart and Allen [1] described a 20-km-diameter concentric multiring structure, named „Silverpit“, ca. 130 km E of the coast of England, centered at 1° 51' E and 54° 14' N. The structure, in Cretaceous chalk and Jurassic shales, is at a present-day depth of 300 to 1500 m below the sea bed. Mapping from detailed 3D seismic reflection data allowed obtaining a detailed structural image of the feature. Multiple rings, similar in appearance to impact craters on Jupiter's moon Europa, are present, and have diameters of ca. 4 to 20 km. The structure also has a small central uplift about 1 km in diameter. The disrupted zone is covered by Tertiary chalk, which constrains the age of the feature between 60 and 65 Ma [1]. Based on the structural interpretation, an impact origin for Silverpit was assumed by [1]. Unfortunately, none of the customary petrographic or geochemical indicators supporting such a proposal were available at the time. Recently, Underhill [2] challenged the impact hypothesis, suggesting that the feature rather formed by salt withdrawal at depth, and that the evidence for a central peak is not unequivocal. He also noted that Silverpit is located on a Tertiary fold axis, a feature interpreted by [3] as possibly being caused by the impact. We studied drill cutting samples from two boreholes for the possible presence of petrographic and geochemical evidence for shock metamorphism or a meteoritic component. We studied 56 polished thin sections made from 42 samples of drill cuttings in three grain sizes (sand, coarse sand, and pebble = 0.5 - 1 cm) from two boreholes located 3 km (well 43/25-1) and 7.5 km (well 43/24-1) from the center of the Silverpit structure. Samples were from the interval between 425 and 836 m depth. A number of lithologies (limestone, fossiliferous limestone, chert, silt- and mudstone, various granitoid- and meta-gneiss-derived lithic and mineral clasts) were sampled by these holes. Thousands of quartz grains, and hundreds of lithic granitic and feldspar particles were scrutinized for shock metamorphic effects, without a single positive recording. Deformation is generally restricted to undulatory extinction in some grains of/with felsic minerals and minor bending and kinking of biotite and muscovite. It is possible that samples from well 43/25-1 contain some partially altered volcanic fragments, but this is still subject of further investigation. In addition, we analyzed most of the same samples also for trace element composition, mainly trying to find enrichments of siderophile elements, in an attempt to detect the presence of a possible meteoritic component. These analyses are still in progress. No unequivocal indication pro or contra an impact origin has been found yet.

Acknowledgments: We are grateful to Phil Allen and Simon Stewart for providing the samples.

**References:** [1] Stewart S.A. and Allen P.J. (2002) *Nature* 418, 520-523. [2] Underhill J.R. (2004) *Nature* doi 10.1038/nature02476. [3] Stewart S.A. and Allen P.J. (2004) *Nature* doi 10.1038/nature02480.

**PETROPHYSICAL CHARACTERISTIC OF  
NEUSCHWANSTEIN EL-6 CHONDRITE.**

T. Kohout<sup>1,2,3</sup>, F. Donadini<sup>1</sup>, L. J. Pesonen<sup>1</sup>. <sup>1</sup> Division of Geophysics, University of Helsinki, Finland. E-mail: tomas.kohout@helsinki.fi. <sup>2</sup> Department of Applied Geophysics, Charles University in Prague, Czech Republic. <sup>3</sup> Institute of Geology, Academy of Sciences of the Czech Republic, Czech Republic

Neuschwanstein meteorite (EL-6) fall occurred on April 6, 2002. Total three meteorite bodies were discovered. Our fragments come from a 1750g body found on July 14, 2002.

Physical properties of Neuschwanstein meteorite were examined using standard petrophysical methods in Solid Earth Geophysics Laboratory, University of Helsinki. First fragment with fusion crust on one side present come from edge part of meteorite body, while the second fragment consists entirely of interior material. Basic petrophysical parameters (density, magnetic susceptibility, NRM, Q-value, magnetic hysteresis parameters) reflect the EL chondrite range determined by meteorite petrophysics database developed by Terho et al.

Neuschwanstein shows quite high anisotropy of susceptibility ( $\chi_{\max} / \chi_{\min} = 1.3$  to  $1.4$ ). Hysteresis parameters points on low coercivity in Neuschwanstein samples. Comparison of the magnetic record of edge and interior fragments shows a definite influence of atmospheric heating on magnetic properties of the edge samples which may reflects possible terrestrial remagnetization or contamination. The Neuschwanstein meteorite will be subject of future more detailed studies.

### COOLING RATE OF OLIVINE MEGACRYST IN THE YAMATO 980459 OLIVINE PHYRIC SHERGOTTITE.

E. Koizumi<sup>1</sup>, T. Mikouchi<sup>1</sup>, M. Miyamoto<sup>1</sup>, A. Monkawa<sup>1</sup>, J. Chokai<sup>1</sup>, and G. McKay<sup>2</sup>. <sup>1</sup>Dept. of Earth and Planet. Science, University of Tokyo, Hongo, Tokyo 113-0033, Japan. E-mail: koi@eps.s.u-tokyo.ac.jp. <sup>2</sup>Mail Code SR, NASA Johnson Space Center, Houston, TX 77058, USA.

**Introduction:** Yamato 980459 (Y98) is a new olivine-phyric shergottite showing several different mineralogical features from other samples in this group. Y98 is a glassy rock showing a porphyritic texture composed of olivine megacrysts and medium-grained pyroxene with abundant mesostasis. In contrast to all other martian meteorites, this meteorite contains no plagioclase. Olivine megacrysts (Fo<sub>85-79</sub>) are euhedral to subhedral and up to 2 mm in size. Olivine (tens to hundreds of  $\mu\text{m}$ ; Fo<sub>79-40</sub>) also exists in the groundmass coexisting with zoned pyroxene (En<sub>81</sub>Fs<sub>17</sub>Wo<sub>2</sub> to En<sub>22</sub>Fs<sub>43</sub>Wo<sub>35</sub>). The mesostasis is glassy, but contains dendritic olivine and pyroxene with other minor minerals [1-2].

**Previous work:** As a previous work, we performed a crystallization experiment and phase calculation with the MELTS program [3]. We found that olivine megacryst in Y98 is possibly a phenocryst because the core composition of olivine megacryst is in equilibrium with the Y98 bulk composition and this was confirmed by the crystallization experiment. These results indicate that the Y98 bulk composition represents a parent melt composition. Furthermore, the core composition of pyroxene is in equilibrium with the rim composition of olivine megacryst (Fo<sub>79</sub>) suggesting that the groundmass pyroxene started crystallizing when the olivine composition reached Fo<sub>79</sub>, which would mark the crystallization of the groundmass olivine. The glassy mesostasis seems to have been formed under a significant undercooling condition suppressing the plagioclase crystallization.

**Cooling rate of olivine megacryst:** In this study, we calculated the cooling rate of olivine megacryst in Y98 considering both fractional crystallization and diffusional modification with a method similar to [4]. Cooling is assumed to be linear from 1460 °C (liquidus of olivine megacryst as estimated by the calculation and experiment) down to 1200 °C (just above the liquidus of plagioclase). We also assumed that olivine crystallization ended around 1360 °C that is the pyroxene liquidus temperature estimated by the calculation. The oxygen fugacity under which olivine crystallized was supposed to be IW+1 as estimated by [5]. According to the calculation result, the best-fit cooling rate of olivine megacryst in Y98 is about 1 °C/hr. This cooling rate suggests that Y98 crystallized at very shallow depth near the martian surface. It is an important issue whether two-stage cooling history (quenching of the magma at some late stage) is required to produce a porphyritic texture with glassy groundmass as observed in Y98. It is not clear whether 1 °C/hr linear cooling can suppress the plagioclase crystallization although our previous experimental work of QUE94201 indicated that the linear cooling at 0.7 °C/hr could produce a porphyritic texture with glassy mesostasis [6]. We are planning to perform a 1 °C/hr cooling experiment of Y98 to verify that this cooling rate can reproduce the Y98 texture.

**References:** [1] Mikouchi T. et al. 2003. *NIPR Symp.*, 82-83. [2] McKay G. et al. 2003. *NIPR Symp.*, 76-77. [3] Koizumi E. et al. 2004. Abstract #1494. 35th Lunar & Planetary Science Conference. [4] Miyamoto M. 1999. *Meteoritics & Planetary Science* 34:A82. [5] McKay G. et al. 2004. Abstract #2154. 35th Lunar & Planetary Science Conference. [6] Koizumi E. et al. 2003. *Geochimica et Cosmochimica Acta*, 67:A227.

**DETONATION NANODIAMONDS INSTEAD OF STARDUST  
IN LABORATORY SIMULATION EXPERIMENTS**

A. P. Koscheev<sup>1</sup> and U. Ott<sup>2</sup>. <sup>1</sup>Karpov Institute of Physical Chemistry, Vorontsovo Pole 10, 105064, Moscow, Russia. E-mail: koscheev@cc.nifhi.ac.ru. <sup>2</sup>Max-Planck-Institut für Chemie, Becherweg 27, D-55128 Mainz, Germany

**Introduction:** Diamond grains of some nanometers in size have been found both in the detonation products of explosions [1] and in primitive meteorites [2]. Meteoritic diamonds (MD) predate the formation of the Solar System and hence can provide information on nuclear and chemical processes near stars and/or in space. However both, the formation of MD and the way of incorporation of trace elements into them are poorly understood. Here we present our results illustrating an exotic «application» of ultradispersed detonation diamonds (UDD) to resolve astrophysical problems.

**Results and Discussion:** We compare results of studies of the properties of UDD and of MD by means of various analytical techniques, including IR and Raman spectroscopy, HRTEM, XRD, thermodesorption mass spectrometry etc. The observed striking similarity between MD and UDD provides a unique possibility to perform laboratory simulations using them as synthetic analogs of presolar nanodiamonds.

We are developing two approaches. In one set of experiments using ion bombardment of UDD, it was shown that ion implantation is a viable mechanism for trapping of noble gases into interstellar diamond grains. The observed isotope fractionation during implantation [3] indicates a need to re-evaluate the composition of supernova components [4]. The data also indicate some elemental fractionation in favor of the lighter noble gases. Thermal patterns of noble gas release during both, pyrolysis and combustion of implanted UDD, were similar to those of MD. These profiles reflect the different sites of trapped atoms in nanocrystals and their depth distribution [5; cf. also 6]. Using UDD preannealed at different temperatures prior ion implantation [7] and measuring active gas release during pyrolysis [7,8] it was shown that the release of implanted noble gases is governed by three processes: thermal escape of atoms trapped at lattice defects, structural transformations in surface layer and such in the bulk of the nanocrystals.

The second approach includes study of the surface chemistry of UDD as analogs of MD by means of IR spectroscopy and mass spectrometry in an attempt to answer the question: can any surface features of nanodiamonds survive the chemical procedure used to extract them from meteorites? Our results revealed that the surface chemistry of UDD after extraction procedure strongly depends on the starting properties of diamond nanograins [9] and hence that the possibility exists to obtain information on the surface chemistry of interstellar grains in space by studying the meteoritic diamonds [10].

**Acknowledgments:** This work was supported by RFBR (grant #03-05-64678) and RFBR-DFG (grant #02-05-04001).

**References:** [1] Greiner N. R. et al. 1988. *Nature* 333:440-442. [2] Lewis R. S. et al. 1987. *Nature* 326:160-162. [3] Koscheev A. P. et al. 2001. *Nature* 412:615-617. [4] Huss G. R. et al. 2000. *Meteoritic & Planetary Science* 35:A79-A80. [5] Koscheev A. P. et al. 2000. Abstract #1551. 31st Lunar and Planetary Science Conference. [6] Verchovsky A. B. et al. 2004. Abstract #1673. 35th Lunar and Planetary Science Conference. [7] Koscheev A. P. et al. 2004. This issue. [8] Koscheev A. P. et al. 2004. *Fullerenes, Nanotubes, and Carbon Nanostructures*. Submitted. [9] Koscheev A. P. et al. 2003. Abstract #1287. 34th Lunar and Planetary Science Conference. [10] Koscheev A. P. et al. 2003. *Meteoritic & Planetary Science* 38:A85.

## RELEASE OF NOBLE GASES DURING PYROLYSIS OF METEORITIC AND SYNTHETIC DIAMONDS: A NEW APPROACH

A. P. Koscheev<sup>1</sup>, M. D. Gromov<sup>1</sup>, N. V. Zaripov<sup>1</sup>, and U. Ott<sup>2</sup>.  
<sup>1</sup>Karpov Institute of Physical Chemistry, Vorontsovo Pole 10, 105064, Moscow, Russia. E-mail: koscheev@cc.nifhi.ac.ru.,  
<sup>2</sup>Max-Planck-Institut für Chemie, Becherweg 27, D-55128 Mainz, Germany

**Introduction:** Thermal release patterns of noble gases during pyrolysis of meteoritic diamonds provide information on the different components of noble gases and on the history of presolar grains [1]. However, the ordinary procedure of stepped heating (100°C steps as a rule) does not allow resolving the fine structure of thermal patterns. We report the first results of continuous measurements of noble gas release during linear heating of the samples in vacuum.

**Experimental:** The diamond samples (0.2-0.8 mg) were heated at a rate 7°C/min up to 1600°C in vacuum. A Ti-getter removed active gases during heating. The released noble gases were measured using a quadrupole mass spectrometer pumped at very low rate through a calibrated orifice. Three types of diamond grains were studied: presolar grains extracted from Murchison meteorite [2], ultradispersed detonation diamonds (UDD) and micro-sized synthetic diamonds both implanted with a noble gas ion mixture [3].

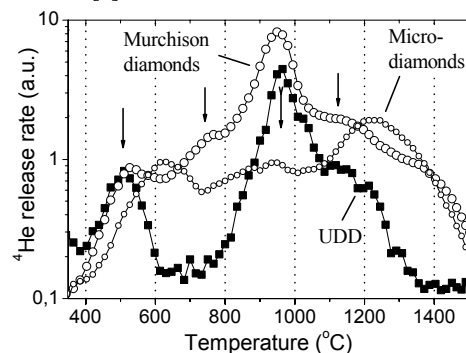


Fig. 1. Thermal release of helium from diamond samples.

**Results and Discussion:** Due to low sample weight, for Murchison diamonds only helium could be measured. The main release peak was at 950°C, with other small peaks near 520, 760 and 1120°C (Fig.1). Most of these features were also observed for ion-implanted UDD, but not for microdiamonds. Kr and Xe were observed in the case of the ion implanted diamonds, with the temperature profiles strongly dependent on the size of diamond grains. For UDD the high-temperature (1200-1500°C) release of Kr and Xe was similar to observations in stepped pyrolysis of meteoritic diamonds [1] and ion implanted UDD [3]. The method developed allows an express analysis of thermal release patterns of noble gases (one day instead of ~2 weeks) with very high temperature resolution. Moreover, release of noble and active gases can be studied simultaneously, which may allow obtaining information on possible mechanisms of noble gas release. Effects on the release profiles of high-temperature annealing of nano-diamonds prior to implantation will also be discussed.

**Acknowledgments:** This work was partially supported by RFBR-DFG (grant #02-05-04001).

**References:** [1] Huss G. R and Lewis R. S. 1994. *Meteoritics* 29:791-810. [2] Merchel S. et al. 2003. *Geochimica et Cosmochimica Acta* 67:4949-4960. [3] Koscheev A. P. et al. 2001. *Nature* 412:615-617.

**ARE CHONDRULES IN THE CB CARBONACEOUS CHONDRITE GUJBA PRIMARY (NEBULAR) OR SECONDARY (ASTEROIDAL)?** A. N. Krot<sup>1</sup>, Y. Amelin<sup>2</sup>, S. S. Russell<sup>3</sup>, and E. Twelker<sup>4</sup>. <sup>1</sup>University of Hawai'i at Manoa, USA. sasha@higp.hawaii.edu. <sup>2</sup>Geological Survey of Canada, Canada. <sup>3</sup>The Natural History Museum, UK. <sup>4</sup>Juneau, USA.

The CB (Bencubbin-like) chondrites are subdivided into the CB<sub>a</sub> (Bencubbin, Gujba, Weatherford) and CB<sub>b</sub> (Hammadah al Hamra 237, QUE94411) subgroups [1]. Both subgroups are characterized by similar O-isotopic compositions, high (60-70 vol%) abundance of Fe,Ni-metal, extreme depletion in moderately volatile elements, and extreme enrichment in <sup>15</sup>N. However, they show some differences as well, including sizes of chondritic components, abundances of CAIs and zoned Fe,Ni-metal grains [1]. Based on detailed mineralogical and trace element studies of chondrules and Fe,Ni-metal grains in CB<sub>b</sub>, it was concluded that they recorded highly energetic thermal event(s) that resulted in complete vaporization of a dusty region of the solar nebula (dust/gas ratio ~10-50 solar). Chemically-zoned metal grains formed by gas-solid condensation in this region [2,3]; chondrules probably formed by gas-liquid condensation before condensation of Fe,Ni-metal [4]. Although condensation has been also invoked for metal grains in the CB<sub>a</sub> chondrites [5], it requires gas with extremely high partial pressures of the siderophile elements (up to ~10<sup>7</sup> CI). Under these conditions, metallic alloy and sulfides condense as liquids [6]. It has been concluded that metal±sulfide and silicate nodules in CB<sub>a</sub> condensed as liquids in a vapor cloud generated in a protoplanetary impact involving a metal-rich body and a reduced-silicate body [5,7]. Here, we report mineralogy and U-Pb isotope studies of chondrules in the CB<sub>a</sub> chondrite Gujba.

Chondrules in Gujba are Fe,Ni-metal-free and have exclusively skeletal olivine textures. They consist of forsteritic olivine (Fa<sub>1-4</sub>), low-Ca pyroxene (Fs<sub>2±2</sub>Wo<sub>3±2</sub>; in wt%, 0.5-16.5, Al<sub>2</sub>O<sub>3</sub>, <0.5, TiO<sub>2</sub>) and high-Ca pyroxene (Fs<sub>2±1</sub>Wo<sub>4±8</sub>; 2-24, Al<sub>2</sub>O<sub>3</sub>, 0.3-1.8, TiO<sub>2</sub>), and glassy mesostasis, and have a narrow range of bulk abundances of refractory lithophile elements (~1-1.6×CI). In contrast, chondrules in the CB<sub>b</sub> subgroup have both skeletal olivine and cryptocrystalline textures and show a large range in bulk abundances of refractory lithophiles (4 <0.01×CI). There is no other chondrite group where chondrules are so drastically different. If the CB<sub>a</sub> and CB<sub>b</sub> chondrites are genetically related, one possible explanation for the observed differences in mineralogy and chemistry of their components is that the latter formed by reprocessing of the latter, i.e., CB<sub>a</sub> chondrules are secondary, not primary nebular products. Our preliminary high precision Pb isotope measurements for multiple fractions from five Gujba chondrules [8] show that three chondrules give a well-constrained U-Pb age of 4562.7±0.5 Ma, MSWD=1.3, whereas two other chondrules yield an errorchron date of 4545.4±3.9 Ma, MSWD=3.6. The latter dates suggest a possible disturbance, post-dating chondrule formation by 15-20 Myr or more, and could be due to shock that resulted in melting of fine-grained interchondrule material and formation of high pressure minerals [9]. A U-Pb isotope study of the CB<sub>b</sub> chondrules is in progress.

**References:** [1] Weisberg M. K. et al. 2001 *MAPS* 36:401-418. [2] Meibom A. et al. 2001. *JGR* 106:32,797-32,801. [3] Campbell A. J. et al. 2001. *GCA* 65:163-180. [4] Krot A. N. et al. 2001. *Science* 291:1776-1779. [5] Campbell A. J. et al. 2002. *GCA* 66:647-660. [6] Ebel D. and Grossman L. 2000. *GCA* [7] [7] Rubin A. E. et al. 2003. *GCA* 67:3283-3298. [8] Amelin Y. et al. 2004. *Goldschmidt Conference* in press. [9] Weisberg M. K. and Kimura M. 2004. #1559. LPSC 35.

**OXYGEN ISOTOPE EXCHANGE IN CAIS AND CHONDRULES: IMPLICATION FOR OXYGEN ISOTOPE RESERVOIRS IN THE SOLAR NEBULA.** A. N. Krot<sup>1</sup>, H. Yurimoto<sup>2</sup>, I. D. Hutcheon<sup>3</sup>, and E. R. D. Scott<sup>1</sup>. <sup>1</sup>HIGP/SOEST, USA. <sup>2</sup>Tokyo Institute of Technology, Japan. <sup>3</sup>LLNL, USA.

On a three-oxygen isotope diagram, compositions of CAIs, AOAs, and chondrules in primitive chondrites plot along a slope of ~1, with CAIs and AOAs enriched in <sup>16</sup>O compared to chondrules [1]. This mass-independent fractionation must have resulted from mixing of the <sup>16</sup>O-rich, solid and <sup>16</sup>O-poor, gaseous reservoirs in the solar nebula [1]. It has been suggested that the initial O-isotopic composition of the solar nebula was uniformly <sup>16</sup>O-rich (<sup>17</sup>O ≤ -20‰) [2-4] and that the <sup>16</sup>O-poor (<sup>17</sup>O > 0‰) gaseous reservoir formed over a life-time of the solar nebula by isotopic self-shielding in the UV photolysis of CO either at the X-point [3] or at the surface of the protoplanetary disk [4]. The alternative models invoke self-shielding of CO in the protosolar molecular cloud [5] or the initial O-isotopic heterogeneity (<sup>16</sup>O-rich solids and <sup>16</sup>O-poor gas) of the solar nebula [6], and predict the very early generation of an <sup>16</sup>O-poor gaseous reservoir in the solar nebula. Such a reservoir could have been recorded by CAIs and chondrules, which represent the first solids formed in the solar nebula. The existence of an <sup>16</sup>O-rich, nebular gaseous reservoir can be inferred from <sup>16</sup>O-rich compositions of the refractory nebular condensates, CAIs and AOAs [7]. The existence of an <sup>16</sup>O-poor, nebular gaseous reservoir ~2-3 Myr after the onset of the CV CAI formation can be inferred from O-isotopic exchange recorded by the CR chondrules [8] and their absolute ages [9]. Coarse-grained CAIs in CVs have heterogeneous O-isotopic compositions: spinel and fassaite are enriched in <sup>16</sup>O, compared to anorthite and melilite. Due to the incomplete melting of the CV CAIs [10], their complex, multistage formation history [11], and the late-stage disturbance of their Al-Mg systematics [12], the nature and timing of this exchange remain controversial. Most CAIs in CRs [13], CHs [14], and COs (3.0) [15] are uniformly <sup>16</sup>O-enriched (<sup>17</sup>O ≤ -20‰). The <sup>16</sup>O-rich, igneous CAIs in CRs have a canonical (<sup>26</sup>Al/<sup>27</sup>Al) ratio of ~5×10<sup>-5</sup> [16], suggesting that they experienced early melting in an <sup>16</sup>O-rich gaseous reservoir. Some igneous CAIs in CRs, CHs, COs (3.0), and all CAIs in CBs [17] are <sup>16</sup>O-depleted (<sup>17</sup>O > -10‰). Two <sup>16</sup>O-poor, Type C CAIs in CRs have low (<sup>26</sup>Al/<sup>27</sup>Al)<sub>0</sub> (<7×10<sup>-6</sup>) [16], similar to those of the CR chondrules [18], suggesting that these CAIs experienced O-isotopic exchange during late-stage (>2.5 Myr after beginning of CAI formation) melting that overlapped with chondrule formation. Another <sup>16</sup>O-poor Type C CAI in CRs has a canonical (<sup>26</sup>Al/<sup>27</sup>Al)<sub>0</sub> ratio [(4.0±1.8)×10<sup>-5</sup>], suggesting the very early, i.e. at the beginning of CAI formation, existence of an <sup>16</sup>O-poor gaseous reservoir, consistent with models of [5] and [6].

**References:** [1] Clayton R. et al. 1977. *EPSL* 34:209-224. [2] Kitamura Y. and Shimizu M. 1983. *Moon Planet.* 29:199-202. [3] Clayton R. 2002. *Nature* 402:860-981. [4] Lyons J. and Young E. 2004. #1923. *LPSC* 35. [5] Yurimoto H. and Kuramoto K. 2002. *MAPS* 37:A153. [6] Scott E. and Krot A. 2001. *MAPS* 36:1307-1319. [7] Krot A. et al. 2002. *Science* 202:1051-1054. [8] Krot A. et al. 2004. #1389. *LPSC* 35. [9] Amelin Y. et al. 2004. *Science* 297:1678-1683. [10] Yurimoto H. et al. 1998. *Science* 202:1874-1877. [11] Hsu W. et al. 2000. *EPSL* 182:15-29. [12] Yurimoto H. et al. 2000. #1593, *LPSC* 31. [13] Aléon J. et al. 2002. *MAPS* 37:1729-1755. [14] Sahijpal S. et al. 1999. *MAPS* 34:A101. [15] Itoh S. et al. 2004. *GCA* 68:183-194. [16] Hutcheon I. et al. 2004. #2124. *LPSC* 35. [17] Krot A. et al. (2001) *MAPS* 36:1189-1217. [18] Marhas K. et al. 2000. *MAPS* 35, A102.

**TYPE C CAIS: NEW INSIGHTS INTO EARLY SOLAR SYSTEM PROCESSES.** A. N. Krot<sup>1</sup>, H. Yurimoto<sup>2</sup>, M. I. Petaev<sup>3</sup>, I. D. Hutcheon<sup>4</sup>, and D. Wark<sup>5</sup>. <sup>1</sup>University of Hawai'i at Manoa, USA. sasha@higp.hawaii.edu. <sup>2</sup>Tokyo Institute of Technology, Japan. <sup>3</sup>Harvard University, USA. <sup>4</sup>Lawrence Livermore National Laboratory, USA. <sup>5</sup>Monash University, Australia.

Coarse-grained, igneous, plagioclase-rich (Type C) CAIs have been initially recognized in the CVs [1,2], and subsequently described in the CRs [3], COs [4], and Ningqiang [5]. Combined mineralogical, Al-Mg and O-isotopic studies of the CR Type CAIs [3,6] revealed that they experienced O-isotope exchange during early and late-stage melting. Such studies of the CV Type C CAIs are scarce: e.g., CAI TTA1-01 in Allende contains <sup>16</sup>O-rich spinel and coarse-grained fassaite, and <sup>16</sup>O-poor melilite, anorthite, and fine-grained fassaite, suggesting O-isotope exchange during incomplete melting [7]. <sup>26</sup>Mg excesses in melilite define a canonical <sup>26</sup>Al/<sup>27</sup>Al ratio of  $5 \times 10^{-5}$ , whereas <sup>26</sup>Al/<sup>27</sup>Al ratio in anorthite ranges from 0 and  $5 \times 10^{-5}$  [7]. Here, we present mineralogical study of the Allende Type C CAIs #100 and #6/1; their O- and Al-Mg isotopic measurements are in progress.

CAI #100 consists of spinel, melilite, coarse-grained and fine-grained fassaite, and anorthite groundmass. Both, coarse-grained melilite and fassaite contain abundant inclusions of anorthite; fassaite often show sector zoning. Melilite grains are pseudomorphed by grossular, monticellite, and forsterite; secondary nepheline is rare. CAI #6/1 consists of the dominant Type C and relict Type B portions. The former is texturally and mineralogically similar to #100. The latter consists of fassaite, melilite, spinel, anorthite, perovskite, and PGE nuggets; fassaite poikilocally encloses melilite. Melilite is replaced along grain boundaries by grossular, forsterite, and monticellite(?). Melilite and anorthite in the periphery of #6/1 are replaced by nepheline and sodalite. Grossular-monticellite-forsterite regions, nepheline and sodalite are crosscut by andradite-bearing veins associated with wollastonite. We infer that Type C CAIs formed by melting of a fine-grained component mineralogically similar to the fine-grained, spinel-rich CAIs [2,5,8], occasionally mixed with a coarse-grained Type A/B-like component. Because #100 and Type C portion of #6/1 contain no relict fassaite and melilite grains, they could have recorded O-isotope composition of the nebular reservoir where they crystallized. Hutcheon and Newton [9] concluded that grossular and monticellite in the Allende Type B CAIs resulted from a closed-system reaction between melilite and anorthite at ~680 C in the solar nebula, at least 5 Myr after crystallization of primary minerals in CAIs. Melilite-anorthite grains in #100 and #6/1 are pseudomorphed by grossular, monticellite, and forsterite, indicating another closed-system reaction:  $3\text{Ca}_2\text{MgSi}_2\text{O}_7 + \text{Ca}_2\text{Al}_2\text{SiO}_7 + 2\text{CaAl}_2\text{Si}_2\text{O}_8 = 3\text{Ca}_3\text{Al}_2\text{Si}_3\text{O}_{12} + \text{CaMgSiO}_4 + \text{Mg}_2\text{SiO}_4$ . Although under equilibrium conditions it occurs below 950 K (for  $\text{Åk}_{70}$ ) and below 700 K (for  $\text{Åk}_{20}$ ), the common presence of melilite-anorthite grains in both CAIs indicates the lack of equilibrium. Our mineralogical observations indicate that replacement of melilite by grossular, monticellite, and forsterite is decoupled from Fe-alkali metasomatic alteration.

**References:** [1] Wark D. 1987. *GCA* 51:221-242. [2] Beckett J. and Grossman L. 1988. *EPSL* 89:1-14. [3] Aléon J. et al. 2002. *MAPS* 37:1729-1755. [4] Itoh S. et al. 2004. *GCA* 68: 183-194. [5] Lin Y. and Kimura M. 1998. *MAPS* 33:435-446. [6] Hutcheon I. et al. 2004. #2124. *LPSC* 35. [7] Imai H. and Yurimoto H. 2000. #1510. *LPSC* 31. [8] MacPherson G. et al. 2002. #1526 *LPSC* 33. [9] Hutcheon I. and Newton R. 1982. *LPSC* 13:491-493.

**CONDENSATION ORIGIN MODEL FOR CHONDRULES.**

G. Kurat<sup>1</sup>, M. E. Varela<sup>2</sup>, E. Zinner<sup>3</sup> and A. Engler<sup>4</sup>. <sup>1</sup>Inst. Geol. Wissensch., Universität Wien, Vienna, Austria. gero.kurat@univie.ac.at. <sup>2</sup>Dept. Geol., UNS-CONICET, B. Blanca, BA, Argentina. <sup>3</sup>Phys. Dept., Washington University, St. Louis, MO, USA. <sup>4</sup>Inst. Mineral. Petrol., Universität Graz, Graz, Austria.

**Old Models:** Chondrules are solidified, once molten silicate droplets. Their chemical and isotopic diversity apparently is incompatible with a simple nebular condensation origin as envisioned by, e.g., [1,2]. This is because it has been thought that liquids condensing from a homogeneous nebular gas should be chemically and isotopically homogeneous and that liquids cannot condense in the solar nebula. Because meteorites contain abundantly objects that obviously must have been fully or partly melted (chondrules, glasses), there is the widespread belief that these objects and in particular chondrules must form from melted solids. There is now growing evidence that liquids can indeed condense from a solar nebula gas, provided the gas/dust ratio is sufficiently low (e.g., 3,4). However, the pre-conception still holds that condensates must be either all liquid or all solid. Here we sketch a way that leads to a simple model for chondrule formation via condensation.

**Observations:** In the course of our studies of glass inclusions in olivines of CC chondrites [5-8] we showed that these glasses must be remnants of a liquid that facilitated growth of the host. Such a liquid is a pre-requisite for growing crystals from the gas phase [e.g., 9], but only a thin film of liquid at the surface of the growing crystal is necessary for that VaporLiquidSolid (VLS) process. Bulk major and trace element patterns of such trapped liquids in olivines are all refractory, have solar relative abundances and clearly signal vapor fractionation and equilibrium with a gas that had solar relative elemental abundances. Matrix glasses of aggregates and chondrules of CC chondrites have trace element abundances indistinguishable from those in glass inclusions, indicating that they are samples of the very same liquid [e.g., 10]. These findings allow us to formulate a new chondrule formation model:

**New Model:** Olivines growing from the nebular gas by the VLS process either stayed single (isolated) or aggregated. The liquid film not only provided an accommodation site for the condensing elements but also a sticking agent for aggregate formation. Small amounts of liquids helped create irregularly shaped olivine (+/- pyroxene) aggregates, elevated amounts forced the formation of droplets of crystal-liquid mush. Solidification of the latter produced chondrules in a single step. Compositional variety is achieved by varying the proportions of olivines and trace element-rich liquid (refractory elements) and by metasomatic elemental exchange between solids and the gas (moderately volatile and volatile elements), e.g., [11]. Isotopic variations (e.g., O) are produced in the same way. Changes in the composition of the gas also allowed the late stage condensation of all-liquid droplets with an advanced chemical composition, the ROP chondrules [12,13]. Thus, chondrules can be produced in one single nebular cooling step with the help of the "universal liquid" [14] and derivatives thereof, no complex mixing of condensates and re-melting is necessary.

**Acknowledgement:** Supported by FWF, Austria (P14938).

**References:** [1] Suess 1949. *Z. Elektrochemie* 53:237. [2] Wood 1962. *Nature* 194:127-130. [3] Herndon and Suess 1977. *GCA* 41:233-236. [4] Ebel and Grossman 2000 *GCA* 64:339-366. [5] Varela et al. 2002a *GCA* 66:1663-1679. [6] Varela et al. 2002b *MAPS* 37, A44. [7] Varela et al. 2003 *GCA* 67:5027-5046. [8] Kurat et al. 2003 34th LPSC. #1733. [9] Givargizov 1987 *Highly Anisotropic Crystals*. Reidel, Dordrecht, 394pp. [10] Varela et al. 2004 *GCA*, submitted. [11] Kurat 1988 *Phil. Trans. R. Soc. Lond.* A325 :459-482. [12] Kurat et al. 1985 16<sup>th</sup> LPSC, 471-472. [13] Engler et al. 2003 34<sup>th</sup> LPSC, #1689. [14] Varela and Kurat 2004, this volume.

**WORLD-WIDE IMPACT STRATIGRAPHY AT THE K-T BOUNDARY: IMPLICATIONS FOR THE CHICXULUB IMPACT ANGLE.** C. Lana<sup>1</sup>, J. Morgan<sup>1</sup>, <sup>1</sup>Earth Science and Engineering, Imperial College London, Consort Road, London, SW7 BP. [c.lana@imperial.ac.uk](mailto:c.lana@imperial.ac.uk)

Over the past few decades, results from stratigraphic, paleontological, geochemical and isotopic investigations have provided a considerable dataset that indicates a temporal link between the Cretaceous-Tertiary (K-T) mass extinction and a world-wide deposition of macro- and microscopic particles with an extra-terrestrial (impact) signature [1]. A large amount of stratigraphic, geochemical and geochronological data, indicate that the 200-km-wide Chicxulub impact structure is the most likely source for the K-T layer [2, 3, 4], although Keller et al. [5] disagree. The K-T layer contains zircons of Pan African basement age, and the size of the ejected particles shows a clear increase towards Chicxulub, suggesting the K-T impact site must be in the same region of the Earth as Chicxulub [2-4].

The impact-related particles (here as K-T impactites) are commonly described as fragments of rock and minerals and melt droplets that were formed from the impacting meteorite, as well as the sedimentary and crystalline target rocks, and ejected around the globe [2-4]. Their world-wide geographical distribution indicates that they possessed significant kinetic energy [6, 7] which, along with their high state of shock, implies that they might have been ejected early in the excavation stage, when high energy release produced shock pressures of tens to hundreds of GPa [6, 7]. Recent studies [7] also suggest that the impactites were accelerated during expansion of a CO<sub>2</sub> and H<sub>2</sub>O vapor plume released from volatile target rocks. There is, however, uncertainty about the angle of impact which, in turn, might have affected the direction of ejection of the particles and their distribution across the globe. Although there is evidence of coarser shocked quartz grains at longitudes to the west of Chicxulub, leading several authors to suggest an impact direction towards the northwest [8], abundance and size of shocked quartz in the known K-T sites have not been systematically quantified.

Here, we present preliminary results of on-going investigation of the distribution, concentration and grain-size of impactites as well as degree of shock metamorphism in quartz from the K-T ejecta horizon exposed across the world. Samples collected so far are from the Western Interior (USA), Spain, Italy and Brazil. The impact related particles were extracted from samples of 100 grams each, following methodology by Montanari and Koeberl [9], and were grouped according to type and grain-size. Shocked quartz grains were mounted in thin sections and had their planar deformation features (PDF) measured for pressure condition estimates at the time of ejection. The results are currently being combined to understand the mechanism in which the quartz and spherules were ejected from the impact site, and how they were deposited across the world. Future work will be directed at establishing the angle of impact based on the overall distribution and abundance of shocked quartz grains.

**References:** [1] Alvarez L. et al. (1980) *Science* 208, 1095-1108; [2] Smit J. (1999) *Ann. Rev. Earth Planet. Sci.* 27, 75-113; [3] Claeys P. (2002) *GSA Spec. Pap.* 356, 55-68; [4] Hildebrand A. (1991) *Geology* 19, 867-871; [5] Keller G. et al. (2004) *PNAS* 101, 3753-3758; [6] Melosh J. (1980) *Ann. Rev. Earth Planet. Sci.* 8, 65-93; [7] Alvarez W. et al. (1995) *Science* 269, 930-934; [8] Schultz P. and D'Hondt S. (1996) *Geology* 24, 963-966. [9] Montanari A. and Koeberl C. (2000) *Lect. Notes Earth Sci.* 364pp.

**PSEUDOTACHYLITE-FRACTURE NETWORK: A KEY STRUCTURE FOR CENTRAL UPLIFT FORMATION IN LARGE IMPACT STRUCTURES** C. Lana<sup>1</sup>, R. Gibson<sup>2</sup>, U. Reimold<sup>2</sup>; <sup>1</sup>Earth Science and Engineering, Imperial College London, Consort Road, London SW7 BP. [c.lana@imperial.ac.uk](mailto:c.lana@imperial.ac.uk); <sup>2</sup>Impact Cratering Research Group, School of Geosciences, University of the Witwatersrand, Private Bag 3, P.O. Wits 2050, Johannesburg, South Africa.

The 80-km-wide Vredefort dome, South Africa, presents a unique opportunity to investigate the deep levels of the central uplift of a very large impact structure. Previous studies have suggested that exposure of progressively older strata in the collar of the dome, and of progressively higher-grade metamorphic rocks toward its center, are consistent with differential uplift, with deepest levels exposed corresponding to pre-impact mid-crust [1, 2, 3]. These studies are confirmed by our recent structural analysis in the core of the dome, which indicates that the amount of impact-related rotation decreases towards the center of the dome [3, 4]. Specifically, they show that the S2 fabric in the outer 3-6 km of the core of the dome is rotated by 90° relative to the S2 fabric found within a 12 km radius of the center [3]. Our structural modeling also indicates that the present asymmetric dips of the collar strata, with layering dipping outward at moderate angles in the southeastern sector but being overturned and dipping inwards in the northwestern sector, and the eccentric distribution of the pre-impact metamorphic isograds around the core of the dome can be reconciled with symmetric rotation of an initially obliquely NW-dipping target sequence during central uplift formation [3]. The remaining question is whether rotation of the deep-seated Archean fabrics was associated with movements along fault zones separating large-scale blocks of crust as observed in similar, but less deeply eroded, impact structures [e.g., 5]. Although the limited exposure of the crystalline basement rocks in the Vredefort dome relative to the collar rocks hampers investigation of large-scale impact-related faulting in the core of the dome, we have identified no obvious fault- or breccia-bounded megablocks. Instead, the continuity of the Archean fabrics suggests that the rotations necessary to create the central uplift were achieved in a more coherent way and that the necessary displacements and rotations were distributed more evenly through the rock volume.

Gibson and Reimold [6] have argued that the bulk, if not all, of the pseudotachylitic breccias in the Vredefort dome formed during the shock compression phase as a consequence of shock melting, with or without a frictional heating component. The presence of a pervasive network of fractures, locally lubricated by these melts, may have provided the necessary temporary strength degradation in the basement and collar rocks during crater modification to allow a large-scale ductile response and to accommodate the differential rotation and slip required for central uplift formation. Although there is no evidence of large slip-magnitudes along major veins of pseudotachylitic breccia, the consistent millimeter- to centimeter-scale displacements of the basement fabrics and collar bedding along the veins suggest that the high-strain deformation could have been distributed as discrete shear in the pseudotachylite-fracture network.

**Reference:** [1] Stevens, G. et al. (1997) *Precamb. Res.* 82, 113-132 [2] Lana, C. et al. *GCA* 68, 623-642. [3] Lana, C. et al. (2003) *MAPS*, 38, 1093-1107. [4] Lana, C. et al., *EPSL* (2003) 206, 133-144; [5] Ivanov, B. et al. (1996) *LPI XXVII*, 589-590. [6] Gibson, R. and Reimold, U. (2003) *LPIC XXXI* 22-23.

**CORROSION OF SOLAR-COMPOSITION FE-BASED ALLOYS: FIRST RESULTS FROM THE NINE CIRCLES EXPERIMENTAL COSMOCHEMISTRY LABORATORY.**

Dante S. Lauretta. Lunar and Planetary Laboratory, University of Arizona, Tucson, AZ, USA. E-mail: lauretta@lpl.arizona.edu

**Introduction:** Iron-based alloys are abundant in many types of primitive meteorites. Since metal is highly reactive, there is potential for significant interaction between it and any external fluid phase. Metal corrosion likely occurred: 1) during the formation and alteration of the first solar system solids, 2) after chondrule formation when volatiles liberated from chondrule melts recondensed, and 3) on chondrite parent bodies as a result of aqueous alteration, thermal metamorphism, and/or shock heating.

Meteoritic metals contain significant amounts of Fe, Ni, Co, P, and Cr [1-4]. The mineralogy resulting from corrosion of such complex metals varies with the conditions of the alteration fluid. Therefore, such phases can provide a record of the metal alteration environment. Thermodynamic calculations can be used to predict metal corrosion products [1-2]. However, such calculations do not take into consideration reaction kinetics, transport mechanisms, and communication between phases, which determine the mineralogy of metal corrosion layers (e.g., [5-7]). Experimental simulation of these environments is required.

**Techniques:** The experimental apparatus contains: a gas-handling system, furnaces, temperature monitors, and a quadrupole mass spectrometer (QMS). An ultra-high purity gas mixture of 1% H<sub>2</sub>S in H<sub>2</sub> at 1 atm total pressure was used. The H<sub>2</sub>S/H<sub>2</sub> ratio corresponds to ~300x the solar S/H ratio. Gas composition was continuously monitored using the QMS. The experiments were performed at 1000, 900, 800, 700, 600, 500, and 400 °C. Temperatures were monitored using type-R thermocouples. Fe-based alloys were custom manufactured to contain 5 at.% Ni, 1% P, 1% Cr, and 0.2% Co, equal to relative CI abundances. Metal foils were exposed to the H<sub>2</sub>S-H<sub>2</sub> gas mixture for 4.5 hours.

**Results:** Reaction kinetics were determined using: 1) S-depletion from the gas phase and 2) total weight gain of the sample. Activation energies determined from these techniques are 52±10 kJ/mole and 44±9 kJ/mole, respectively. These values are slightly lower than those determined by sulfurization of pure Fe under similar conditions [5]. Detailed kinetic behavior is determined by monitoring the abundance of H<sub>2</sub>S throughout the experiment. The reaction rate is most rapid immediately after the foil is introduced to the hot zone. At 400 – 700 °C the reaction rate decreases rapidly and reaches a steady-state value after less than one hour of reaction time. At 800 and 900 °C a similar behavior is observed but the reaction rate continues to decrease throughout the experiment. At 1000 °C, above the Fe-FeS eutectic, the reaction rate is constant for 1.5 hours then decreases.

The sample formed at 1000 °C had a rounded droplet morphology. Troilite contained 0.2 – 1.3 (at.%) Cr, 0.2 – 0.6% Ni, and 0.1 – 0.2% Co. In addition schreibersite contained 0.2 – 1.2% S, 2.4 – 4.1% Co, and 8.0 – 12% Ni. The remnant metal contained 1.3% P, 3.9% Co, and 20% Ni, balance Fe.

**References:** [1] Lauretta et al. 2001 *Geochimica et Cosmochimica Acta* **65**, 1337. [2] Lauretta and Buseck 2003 *Meteoritics and Planetary Science* **38**, 59. [3] Rambaldi and Wasson 1981 *Geochimica et Cosmochimica Acta* **45**, 1001. [4] Zanda et al. 1994 *Science* **285**, 1846. [5] Lauretta et al. 1996 *Icarus* **122**, 288. [6] Lauretta et al. 1997 *Science* **277**, 358. [7] Lauretta et al. 1998 *Meteoritics & Planetary Science* **33**, 821.

**Acknowledgments:** Supported by NASA grant NNG04GF65G.

**DUST-BUSTER ISOTOPE TOF-MS FOR STARDUST**

Typhoon Lee<sup>1</sup>, W.F. Calaway<sup>2</sup>, C.Y. Chen<sup>1</sup>, J.F. Moore<sup>2</sup>, M.J. Pellin<sup>2</sup>, and I.V. Veryovkin<sup>2</sup> <sup>1</sup>Inst. Earth Sci., Academia Sinica, Box 1-55, Nankang, Taipei, Taiwan 115. <sup>2</sup>Materials Sci. Div., Argonne Nat'l Lab., Argonne, IL 60439 USA.

Academia Sinica (AS) and Argonne National Lab (ANL) have entered into a collaboration to develop a high sensitivity time-of-flight mass spectrometer (TOF MS). It aims to measure as many isotope ratios as possible over a wide mass range in individual grains collected by the STARDUST spacecraft during its fly-by of comet Wild-2. A new MS called DUST-BUSTER is being built at AS based on the new TOF MS design developed at ANL. An instrument of similar design, named SPIRIT, is already in operation at ANL. A 157 nm (=7.9 eV photon) F<sub>2</sub> laser with 1 mJ/pulse energy running at 100 Hz was used as the source of photons. It photoionizes secondary neutral atoms sputtered from the grain surface by a primary Ar<sup>+</sup> ion beam. This high sensitivity TOF MS has a transmission of >95% resulting in high useful yields (>12% demonstrated for Mo). Here we report preliminary results for measuring the isotope ratios of several major elements (e.g. Ti and Ca) in refractory minerals such as sphene (CaTiSiO<sub>5</sub>).

To test the precision of analog data collection (i.e. the integration of detector current over time-of-flight), we used a 1 μA primary ion beam (100 μm across). This is suitable for large signals because the integrated charge is proportional to the total number of ions. The short term (same day) reproducibility for Ti 46, 47, and 50 relative to 48 were within 1% (1 σ). The deviations from absolute ratios as measured at AS by thermal ionization mass spectrometry (TIMS) were less than 10 %.

The second experiment tested the ion counting method by reducing the Ar beam to < 1 nA and < 10 μm in width. Data acquisition using counting works best when analyzing low intensity signals from small particles. It improves the signal-to-noise ratio since ions can be separated from analog noise by discrimination. In counting mode, we accumulated spectra consisted of 5120 averages with the most intense signal being <0.1 count per average. Typical reproducibility was 5-10% (1 σ) with hydride remaining a major interference. Pre-cleaning the target surface before data acquisition reduces hydride formation and increases photo-ion yield.

A major difficulty in analyzing comet dust is that individual isotopically unique grains are so small that often only one analysis per grain is possible. With the high sensitivity of laser post-ionization TOF MS simultaneous precise measurements on all species that are photoionized are possible. For instance, TiO photo-ions were more abundant than Ti photo-ions when using 157 nm UV. Therefore if Ti and TiO (even TiO<sub>2</sub>) all yield the same isotope effects then the measurements are more likely to be correct since interferences in different mass ranges should cause different artifacts in general. Similarly, some Ca isotope ratios may be measured from both Ca and CaO.

This work is supported by the U. S. Department of Energy, BES-Materials Sciences, under Contract W-31-109-ENG-38, and by NASA under Work Orders W-19,895 and W-10,091. Grants from Academia Sinica and National Science Council in Taiwan are also essential for this research.

### FeO-RICH XENOLITHS IN THE STAROYE PESYANOE AUBRITE.

C. A. Lorenz<sup>1</sup>, M. A. Ivanova<sup>1</sup>, G. Kurat<sup>2</sup>, F. Brandstaetter<sup>2</sup>.  
<sup>1</sup>Vernadsky Institute of Geochemistry, Moscow, Russia. c-lorenz@yandex.ru. <sup>2</sup>Naturhistorisches Museum, Vienna, Austria. gero.kurat@univie.ac.at

**Introduction:** The Staroye Pesyanoë aubrite (SP) is a polymict gas-rich breccia, consists predominantly of enstatite but contains also abundant glass spherules. We analysed four polished sections (2.5 cm<sup>2</sup> total sample area) with optical microscopy, ASEM, and EMP, and found six non-aubritic, FeO-rich mineral and lithic clasts, possibly related to ordinary chondrites (OC) and carbonaceous chondrites (CC). The xenoliths demonstrate accretion of chondrite-like particles onto the surface of the aubrite parent body (APB). However, the flux of interplanetary dust seems to have been different from that on the HED parent body and Earth by composition and intensity. It could indicate that the APB sampled the dust at a different time or moved through a different region of the Solar System than did the HED parent body and the Earth.

**Results:** In total, three olivine xenocrysts (15-30 µm) and three xenoliths (~ 50 µm each) were found – corresponding to an area fraction of ~ 3.6\*10<sup>-5</sup>. The three small olivine xenocrysts (Fo<sub>78</sub>–Fo<sub>88</sub>; Fe/Mn=40) are angular and contain tiny inclusions of Cr- and Mn-poor troilite. One xenolith consists of olivine Fo<sub>84</sub>, troilite and some albitic feldspar (Ab<sub>83</sub>An<sub>12</sub>) or glass. The other FeO-rich xenolith consists of two anhedral grains of orthopyroxene (En<sub>87</sub>Wo<sub>0.2</sub>; Fe/Mn=22) and augite (En<sub>57</sub>Wo<sub>35</sub>) in a glassy mesostasis of feldspathic composition (Ab<sub>83</sub>An<sub>15</sub>), containing also tiny troilite grains. All silicates are poor in minor elements. Occasionally, FeO-rich pyroxene and augite are Cr<sub>2</sub>O<sub>3</sub>-rich (up to 1.34 wt%). The third xenolith is a carbonaceous chondrite clast, consists mainly of fine-grained phyllosilicate matrix into which forsterite and troilite grains are embedded.

**Discussion:** The xenocrysts and xenoliths have no features of shock, therefore, accretion onto the SP PB must have taken place with very low relative velocity. The angular shape, compositional homogeneity and absence of reactions between the xenocrysts/xenoliths and the aubrite material suggest that SP did not experience thermal metamorphism after the FeO-rich material was mixed in. The compositions of FeO-rich olivine xenocrysts in SP correspond to that of H-chondrites by both major and minor element abundances. However, our xenoliths are less magnesian and pyroxene-rich than a FeO-rich xenolith recently described from SP [1] and FeO-rich materials found in other aubrites [2], which also correspond to H chondrites with the exception of an oxidized LL-like clast described from Cumberland Falls [3]. We suggest that the accretionary flow onto the APB (-s) was less intensive and had a different abundance ratio of CC/OC (~ 0.4) than that on Earth and the HED PB (CC/OC ~ 100-1000) [4, 5]. It could mean that accretion onto the APB occurred at a different time piece than onto the HED PB, or that APB orbited through an unusual region of the Solar System.

**References:** [1] Ivanova M. A. et al. 2002. LPSC 33, Abs. #1080. [2] Kimura M. 1993. Proc. NIPR Symp. Antarct. Met. 6, 186-203. [3] Kallemeyn G., Wasson J. 1985. GCA 49, 261-270. [4] Kurat G. et al. 1994. GCA 58, 3879-3904. [5] Zolensky M. et al. 1996. MAPS 31, 518-537.

### ARE CHONDRITES OLDER THAN ACHONDRITES? – THE TALE OF AL-26.

K.L. Lundgaard<sup>1</sup>, M. Bizzarro<sup>1,2</sup>, J.A. Baker<sup>1</sup>, and H. Haack<sup>2</sup>.

<sup>1</sup>Danish Lithosphere Center, University of Copenhagen, Øster Voldgade 10, DK-1350 Copenhagen K, Denmark. E-mail:

kl@dlc.ku.dk. <sup>2</sup>Geological Museum, University of Copenhagen, Øster Voldgade 5-7, DK-1350 Copenhagen K, Denmark.

**Introduction:** Chondrites are generally believed to represent the precursor materials from which planets, Moons, and a diverse suite of achondrite parent bodies accreted. We have measured <sup>26</sup>Mg in CAIs and chondrules from Allende (CV3) [1,2] and in whole rock and mineral separates from the eucrite Juvinas [3]. These new high precision chronological data and absolute Pb-Pb ages [4] of chondrules and CAIs suggest chondrule formation lasted at least 1 Ma and was still ongoing at the time when the HED parent body accreted.

**Results:** We find (<sup>26</sup>Al/<sup>27</sup>Al)<sub>0</sub> ratios for Allende CAIs in the range 3.5–6.3 × 10<sup>-5</sup> suggesting that the Allende CAIs formed over a period of 0.6–0.2 Ma. Two aluminium rich chondrules and four out of seven ferromagnesian chondrules from Allende showed excess <sup>26</sup>Mg with (<sup>26</sup>Al/<sup>27</sup>Al)<sub>0</sub> ratios in the range from 1.7–4.8 × 10<sup>-5</sup>. These data suggest that the Allende chondrules formed over a period of 1–0.5 Ma and that the oldest chondrules are as old as the oldest CAIs.

We have also found a <sup>26</sup>Mg\* excess in mineral separates from the eucrite Juvinas. If <sup>26</sup>Al was homogeneously distributed in the nebula these data suggest that the HED parent body accreted while chondrules were still forming.

**Implications for early solar system chronology:** The overlap in formation ages for the chondrules and CAIs in Allende inferred from our data removes a previous concern that CAIs would no longer be present in the nebula by the time the chondrules formed. The extended duration of the chondrule formation event makes it possible that chondrules in different parent bodies formed at different times thus explaining the different abundances of the early formed CAIs in different parent bodies. This would imply that chondrules in ordinary chondrites formed later than the chondrules in Allende.

Our data also has several significant implications for the formation of achondrite parent bodies: 1) <sup>26</sup>Al appears to have been the dominating heat source in the early Solar System. If <sup>26</sup>Al was homogeneously distributed throughout the solar system this implies that the chondrite parent bodies must have accreted later than the achondrite parent bodies in order to escape heating and differentiation. 2) If achondrites come from parent bodies that accreted prior to the formation of chondrules in ordinary chondrites then we may have no samples of the precursor materials. Although ordinary chondrites are the most abundant type of meteorite falling on Earth today they may be different from the material ~150 achondrite parent bodies accreted from.

**References:** [1] Baker J.A. et al. (2004) *Goldschmidt Conf. Abstract #1305*. [2] Bizzarro M. et al. (2004) *Goldschmidt Conf. Abstract #896*. [3] Lundgaard, K.L. et al. (2004) *Goldschmidt Conf. Abstract #250*. [4] Amelin, Y. et al. (2004) *Goldschmidt Conf. Abstract #958*.